Article Identifier
DOI: 10.22032/dbt.58890
URN: urn:nbn:de:gbv:ilm1-2023isc-091:6

60th ILMENAU SCIENTIFIC COLLOQUIUM
Technische Universität Ilmenau, 4 – 8 September 2023
URN: urn:nbn:de:gbv:ilm1-2023isc:1

RELAXATION BEHAVIOR OF (CYLINDRICAL) HELICAL COMPRESSION SPRINGS

Johannes Schleichert, Ulf Kletzin

Department of Mechanical Engineering, Institute for Design and Precision Engineering
Machine Elements Group, Technische Universität Ilmenau, Germany

ABSTRACT

This paper deals with the relaxation behavior of helical compression springs made out of different types of spring steel wire. The starting point of the examinations marks the creep and relaxation behavior of similar preprocessed wires prior to the cold forming under torsional stress. In this context the main influencing factors regarding creep deformations and relaxation losses are discussed and the particular findings contrasted, which allows for transfer factors to be deducted. The mathematical models forming the evaluation basis of the experimental data are based upon the NORTON-BAILEY creep law and utilized to determine creep specific characteristics and identify material constants. Doing so enables the deviation of calculating instructions to estimate the relaxation losses of helical compression springs based on numerous influencing factors. Applying those calculation methods facilitates the deduction of relaxation figures as well as recommendations regarding the manufacturing process in order to achieve springs with favorable relaxation behavior.

Index Terms - *relaxation, creep, spring steel wire, helical compression spring, pretorsioning, presetting*

1. MOTIVATION AND APPROACH

Reproducibility and accuracy of the machine element "spring" have to meet ever-increasing demands. During their life cycle, springs are often exposed to high amounts of mechanical stress and increased surrounding temperatures. This causes creep processes in the material, which can impair the function of the springs or even lead to their failure. The European standard EN 13906-1 provides a selection of relaxation figures which fail to meet today's demands: they date back to 1960's, have largely unknown experimental conditions and are only valid for a relaxation time of 48 hours [1]. It is assumed that no significant creep deformations will take place after this amount of time, which is not accurate. In order to predict these phenomena and to keep them as small as possible, knowledge of how they can be mathematically engaged is required as well as carrying out experiments in which different influencing variables are varied and with whom creep-related material parameters can eventually be identified.

2. BASIC KNOWLEDGE REGARDING CREEP PHENOMENONS

The phenomenon that solid materials are already beginning to show plastic deformations over time when being charged with stress conditions below the elastic limit is called "creep". The

most important factor for creep processes besides the stress present in the material is the ambient temperature, which a sample or a component is exposed to. The reason therefor being that creep processes are thermally activated space exchange events, whose extent is strongly temperature-dependent. Creep effects can be separated into three basic mechanisms [2]:

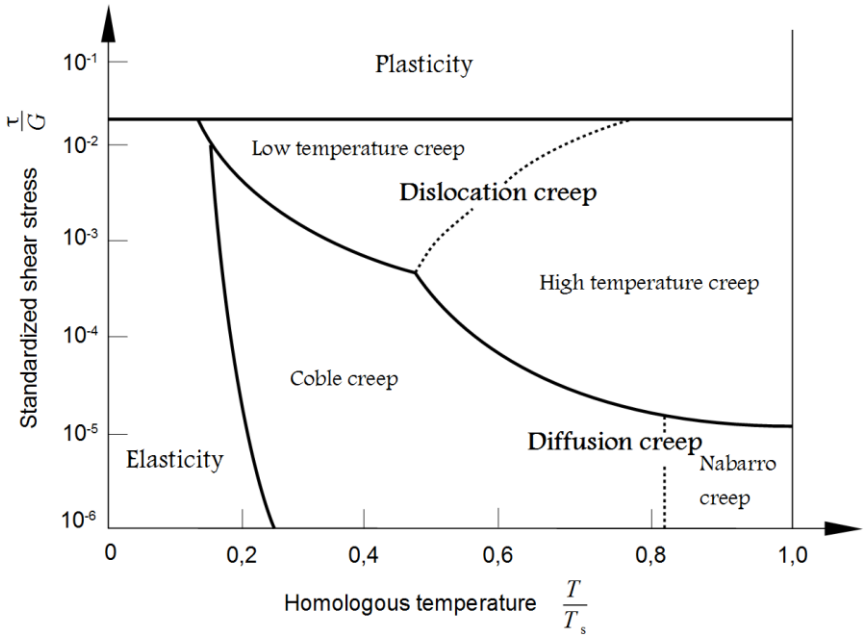

Figure 1:
Qualitative Deformation-Mechanism Map [2][3]

- Dislocation creep (Dislocations can avoid obstacles/blockages by climbing (attaching/sending out vacancies))
- Grain boundary sliding (Grains slipping of each other; not depicted, occurs simultaneously with dislocation creep at high levels of creep stress)
- Diffusion creep (Movement of vacancies in the material)

In the illustrated ASHBY diagram (**figure 1**), the shear stress at hand is normalized to the shear modulus and plotted against the ratio of the creep/relaxation temperature T to the melting temperature T_s. A temperature limit based on the melting temperature T_s frequently referred to in literature above which metallic materials begin to creep is $0{,}4 \cdot T_s$. While this can act as a sufficient guideline for many metals, some materials – including spring steel wires – show pronounced creep phenomena even at significantly lower temperatures [4]. Spring wire steels can thus be assigned to the low temperature creep, which is located in the area of the dislocation creep. The time course of creep processes is usually displayed with the aid of the resulting creep rate (strain rate) $\dot{\varepsilon}$, which corresponds to the initial strain speed $\dot{\varepsilon}_0$ at the beginning of the creep process. The course of the creep rate, as seen in **figure 2**, can be subdivided into three characteristic areas of varying duration and practical relevance [2][5]:

- Primary creep – the initially high creep rate steadily decreases as a result of strain hardening processes
- Secondary creep – the creep rate reaches a minimum value, dynamic equilibrium between strain hardening and softening processes
- Tertiary creep – the creep rate steadily increases until fracture due to irreversible impairment processes, hardly any significance in practice

The shift of this so-called "creep curve" for higher temperatures towards greater amounts of strain rate is approximately the same behavior which can be observed with increasing stress.

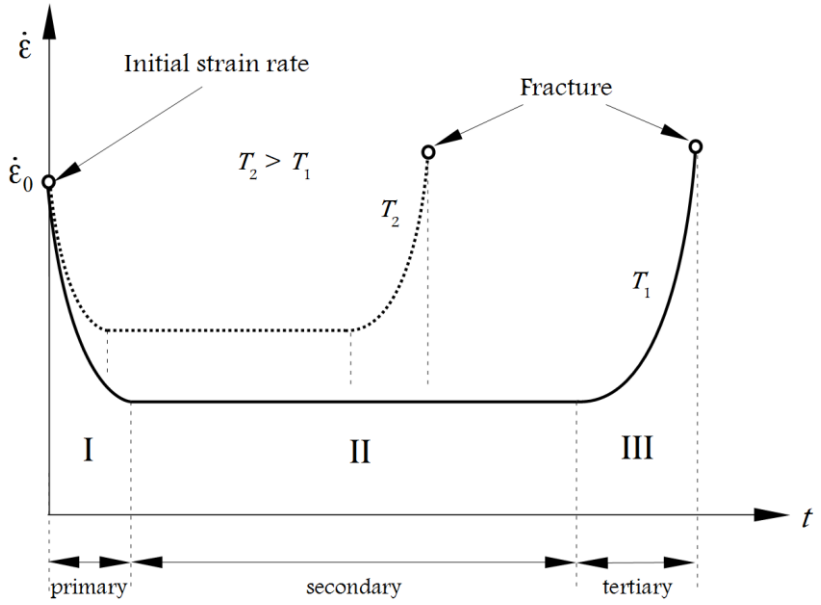

Figure 2:
Course of the strain rate (creep rate) over time regarding creep processes exposed to a constant level of stress [2]

The first key phase is the one of primary creep, which connects immediately to the elastic deformation. How quickly this area is giving way to the following, depends not only on the temperature, but also on the mechanical stress.
In practice, creep effects can manifest themselves in two different ways. On one hand, an increase in deformation can be observed while applying a constant external load. This phenomenon is referred to as "creep". If, on the other hand, a constant deformation is being implemented, the result is a reduction of the mechanical stress prevailing in the material respectively of the reaction forces/moments, which the component or the test body exerts on its contact elements. This phenomenon is referred to as "relaxation".

3. MATHEMATICAL APPROACH

There are a number of different approaches regarding the mathematical evaluation of creep effects. For torsional stress, which is the relevant stress situation when it comes to helical springs, the three most common ones were adapted by Prof. KOBELEV in [5] and [6]. Based on this, the relations provided by the NORTON-BAILEY law, which is by far the most frequently used creep law, covering a large stress and temperature range, are used in this paper by applying them to the obtained experimental results. Creep processes occurring on wires loaded with torsional stress cause an increase of the twist of the wire – expressed via the torsion angle φ(t) – over time, which can be described as [7]:

$$\varphi(t) = \frac{t^k}{k} \cdot l \cdot c_\tau \cdot \frac{2^{2m+3}}{d^{3m+4}} \cdot \left(\frac{M_t^0}{\pi} \cdot \frac{3m+4}{m+1} \right)^{m+1} \tag{1}$$

l represents the length of the twisted piece of wire, d the wire diameter and M_t^0 the temporally constant torsional moment, which loads the wire. m and k are creep related constants, which are dependent upon the material respectively the testing/practical conditions and have to be determined experimentally. k complies with the prevailing creep phase (**figure 2**) and reaches the value 1 in the secondary phase, whereas in the primary phase $0 < k < 1$ is valid. The variable m provides information on the creep mechanism at hand. In the case of diffusion creep, m equals 0, for grain boundary sliding $0 < m < 1$ holds true and regarding dislocation creep, m is located between 3 and 6 (see **figure 1**) [5]. c_τ is an auxiliary parameter, which combines another three

material-dependent creep constants while also being a function of m and k as well as taking the influence of the surrounding temperature T into account [7]:

$$c_\tau(k,m,T) = \frac{\bar{\gamma}}{\bar{t}^{k-1} \cdot \bar{\tau}^{m+1}} \cdot e^{\left(-\frac{Q_c}{R_c \cdot T}\right)} \tag{2}$$

The other variables in equation 2 are:

- $\bar{\gamma}$ – creep related strain parameter
- $\bar{t}$ – creep related time parameter [s]
- $\bar{\tau}$ – creep related stress parameter [Pa]
- Q_c – activation energy of creep processes [J/mol]
- R_c – universal gas constant [1/mol K]
- T – absolute temperature [K]

When, on the other hand, considering relaxation processes, the over time decreasing torsional moment of the wire $M_t(t)$ needs to be described. Regarding torsional stress, the NORTON-BAILEY creep law delivers a hypergeometric function, which is dependent on the torsional moment before the start of the relaxation process M_t^0 [6]:

$$M_t(t) = {}_2F_1\left(\frac{1}{m}, \frac{4}{m}; \frac{4+m}{m}; -\frac{c_\tau \cdot G \cdot \tau_0^m \cdot m \cdot t^k}{k}\right) \cdot M_t^0 \tag{3}$$

G represents the shear modulus and τ_0 the maximum shear stress before the start of the relaxation process. For certain, fix values of m, this expression can be simplified into an elementary equation. Within the framework of the evaluated experiments, $m = 4$ has led to a good correlation between the experimental results and the mathematical model. The corresponding function, now independent of m, is [7]:

$$M_t(t) = M_t^0 \cdot \frac{k}{3} \cdot \frac{\left(1 + \frac{4 \cdot c_\tau \cdot G \cdot \tau_0^4 \cdot t^k}{k}\right)^{\frac{3}{4}} - 1}{c_\tau \cdot G \cdot \tau_0^4 \cdot t^k} \tag{4}$$

$m = 4$ is equivalent to the fact that the predominant creep mechanism is dislocation creep, which seems reasonable in view of **figure 1** considering the high levels of stress at hand. For helical compression springs, relaxation means that the spring is compressed by a fix spring deflection s and consequently the axial spring force $F(t)$, which the spring exerts on its contact area, decreases.
The spring force and the torsional moment loading the wire are directly proportional to one another and are idealized (which means without consideration of the unsymmetrical torsional stress distribution in the wire cross section of a helical compression spring. This can be argued to be justified, considering all of the experiments are carried out with static load) linked via the following relation, as a function of the mean coil diameter D:

$$F(t) = \frac{2M_t(t)}{D} \tag{5}$$

Consequently, the resulting correlations for relaxation processes of helical compression springs with a constant wire diameter and constant mean coil diameter, take on a very similar form compared to those for wires under torsional stress. The general relation describing the decrease

of the spring force $F(t)$ over time as a function of the spring force at hand before the start of the relaxation process F_0 hence results in [5][6]:

$$F(t) = {}_2F_1\left(\frac{1}{m}, \frac{4}{m}; \frac{4+m}{m}; -\frac{c_\tau \cdot G \cdot \tau_0^m \cdot m \cdot t^k}{k}\right) \cdot F_0 \tag{6}$$

Correspondingly, for $m = 4$ [5][6]:

$$F(t) = F_0 \cdot \frac{k}{3} \cdot \frac{\left(1 + \frac{4 \cdot c_\tau \cdot G \cdot \tau_0^4 \cdot t^k}{k}\right)^{\frac{3}{4}} - 1}{c_\tau \cdot G \cdot \tau_0^4 \cdot t^k} \tag{7}$$

4. EXPERIMENTAL RESULTS

The experiments carried out consist of creep tests with spring steel wires, relaxation tests with spring steel wires and relaxation tests with helical compression springs. The majority of the tests were conducted with spring steel wires under torsional stress because of their considerably easier implementation while being very close to the actual stress situation of the component "spring". The results obtained from the tests on wires are opposed to the spring-based relaxation tests and compared with each other. The following types of spring steel wires with wire diameter of 2, 3 and 6 mm have been part of the creep and relaxation tests:

- Oil hardened and tempered spring steel wire, specifically VDSiCr and VDSiCrV
- Patented drawn spring steel wire
- Stainless spring steel wire, specifically material no. 1.4310

Each of the wire types has been exposed to 2-3 well-established levels of heat treatments (HT) prior to the creep experiments, while the surrounding temperatures have been varied from 40°C up to 160°C (dependent on the temperatures that the correspondent springs will be exposed to in service and according to those mentioned in the European standards). Another variation parameter comes in form of a pre-torsion (PT) of the wires during which they are exposed to a certain amount of stress > $\tau_t^*{}_{0,04}$; this is done to counterfeit the process step of (cold) pre-setting of compression springs.

4.1 Creep tests with spring steel wire

In the context of creep tests on wire, "creep" always means a further increase in the torsion angle $\varphi(t)$ beyond the angle that results from the preset amount of torsional stress, lying entirely within the elastic range – which means below the torsional yield point $\tau_t^*{}_{0,04}$. Within the scope of the experiments, the torsion angle has been continuously measured over time intervals ranging from 24 to 300 hours. **Figure 3** shows the torsional creep device which was designed especially for carrying out these experiments. For better visualization, the subsequently shown curves are calculated curve fits based on the measuring points up to a creep time of 100 hours and are displayed as the percentaged (standardized) increase of the elastic shear strain γ resulting from creep deformation (*equal to the percentaged increase of the elastic torsion angle φ*).

(a) open, with built-in wires

(b) closed, running a test

Figure 3: Torsional creep device

Figure 4 shows creep curves of VDSiCrV wire (d = 3 mm, HT: 350°C/30min) for different levels of creep stress and creep temperature. The expected pattern of increasing creep deformation with growing amounts of creep stress as well as creep temperature presents itself quite clearly with the applied creep stress being predominant. Also, the slopes of the curves increase with the level of creep stress.

In **Figure 5**, creep curves of 250°C/30min-HT Pb-patented wire are displayed for various amounts of creep stress and pre-torsion stress at a creep temperature of 120°C. The positive effect of pre-torsion can be seen – even though it is far less potent as for the oil hardened and tempered as well as the stainless spring steel wires. For the latter (d = 3 mm, HT: 200°C/30min), **Figure 6** contains creep curves for various amounts of creep temperature at 686 MPa creep stress. The pre-torsioning reduces the creep deformation significantly. Because of the very low torsional yield point of the 1.4310-wire – especially with HT at below 200°C – the material tends to consolidate considerably more through the pre-torsion process than other types of spring steel wire.

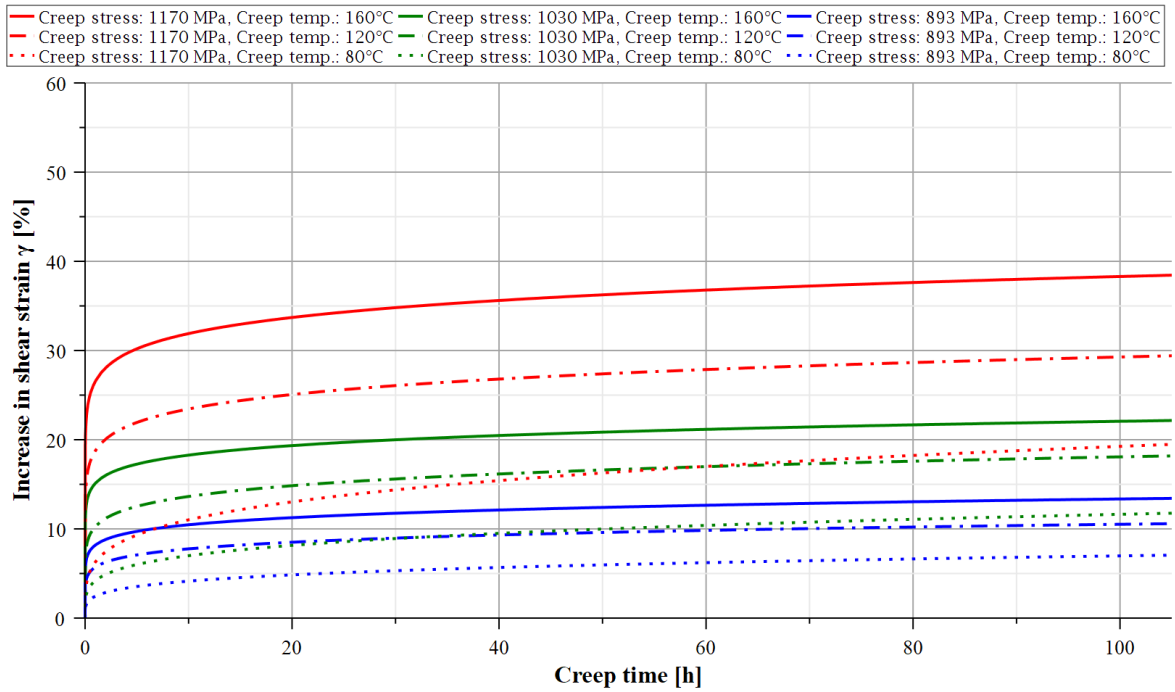

Figure 4: Creep curves of **VDSiCrV** wire (d = 3 mm), **350°C/30min** heat-treated and with **1450 MPa** pre-torsion stress with various amounts of creep stress and temperature

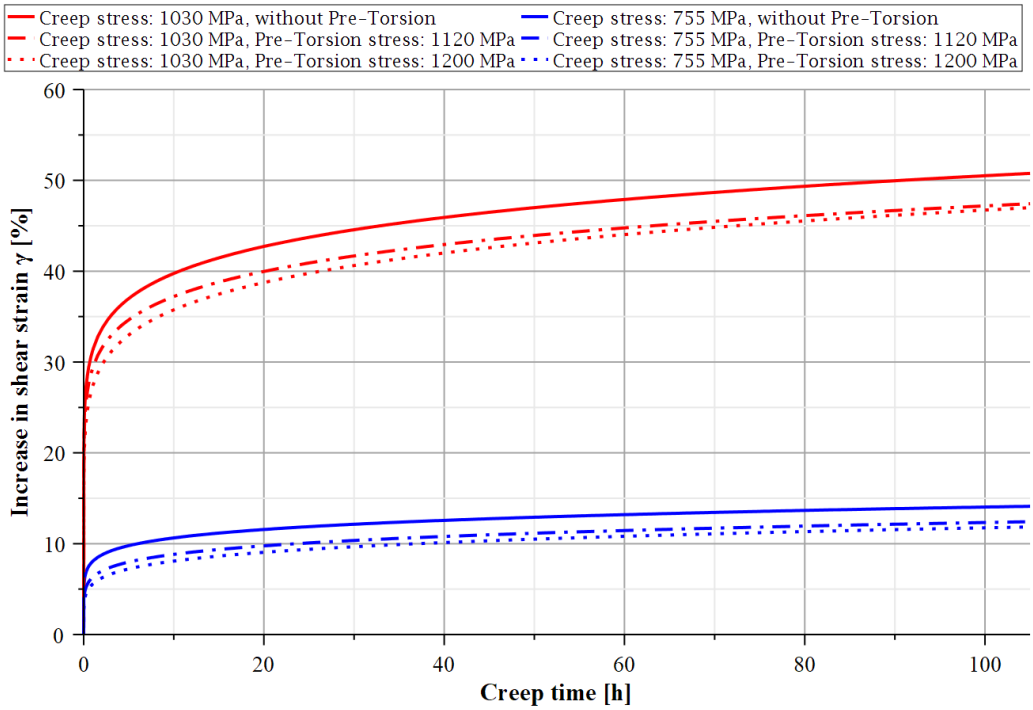

Figure 5: Creep curves of **Pb-pat.** wire (d = 3 mm), **250°C/30min** heat-treated, with various amounts of pre-torsion and creep stress, at **120°C** creep temperature

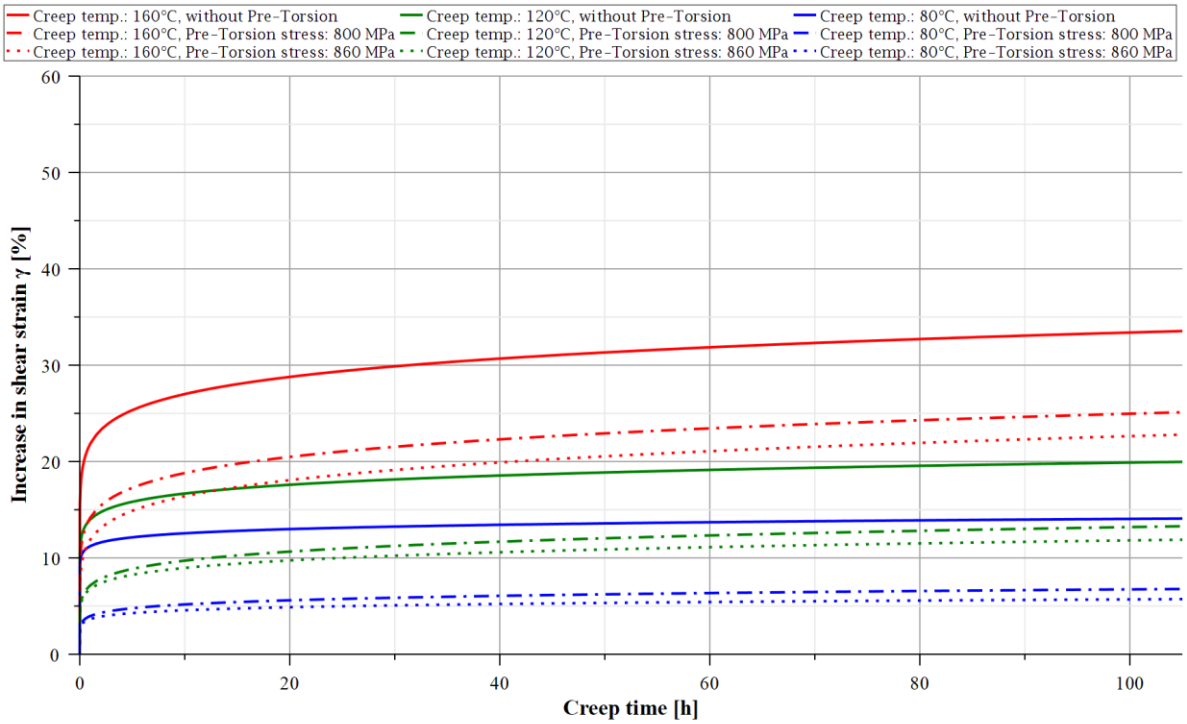

Figure 6: Creep curves of **1.4310** wire (d = 3 mm), **250°C/30min** heat-treated, with various amounts of pre-torsion stress and creep temperatures, at **686 MPa** creep stress

4.2 Relaxation tests with spring steel wire

According to the European standard EN 13906-1 [1] the relaxation is usually determined after 48h. In the context of the relaxation experiments carried out, the decline of the torsional moment is determined as a function of time for test points in the interval 0 – 96h, more precisely at 0, 5, 24, 48 and 96h.
The four temporal measuring points of the reduced torsional moment $M_t(t)$, as well as the curve fits, calculated by means of **equation 4**, are displayed by plotting the relaxation loss over the relaxation time, which is precisely "1 – moment ratio $M_t(t)$ / M_t^0" (for each wire, M_t^0 is measured at the start of the relaxation tests):

$$\text{Relaxation loss [\%]} = (1 - \frac{M_t(t)}{M_t^0}) * 100\ \% \qquad (8)$$

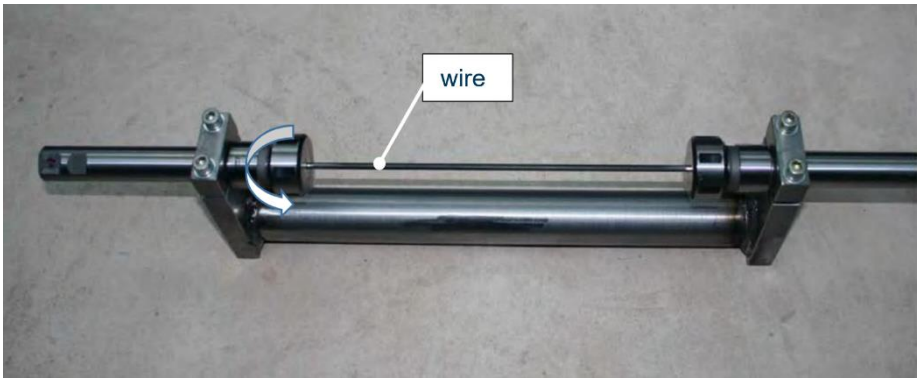

Figure 7: Wire relaxation device

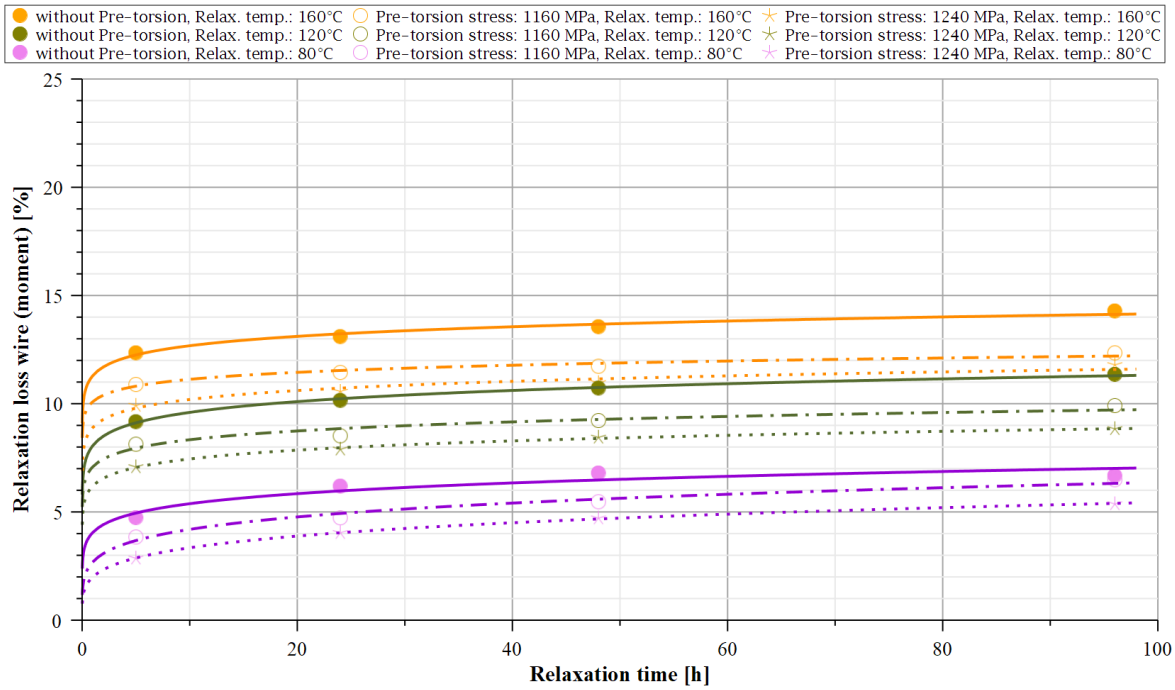

Figure 8: Relaxation curves of **VDSiCr** wire ($d = 3$ mm), **350°C/30min** heat-treated, with various amounts of creep temperature and pre-torsion stress, at **900 MPa** relaxation stress

Figure 7 shows the wire relaxation device while **figure 8** showcases exemplary relaxation curves of VDSiCr wire ($d = 3$ mm, HT: 350°C/30min) for various amounts of creep temperature and pre-torsion stress at a fixed level of relaxation stress. Increasing relaxation temperature results in increasing relaxation losses whereas increasing pre-torsion stress results in decreasing relaxation losses. These observations confirm the assessments of the creep tests and hold true for the other examined wire types as well.

4.3 Relaxation tests with helical compression springs

Analogous to the procedure for relaxation tests with wires, test points were once again determined in the interval from 0 – 96h, specifically at 0, 5, 24, 48 and 96h. In this case, the decrease in spring force represents the measured variable of interest. Relaxation tests with helical compression springs (HCS) have been carried out for springs spanning four spring indexes ($w = 3$, 5, 8 and 12), heat treatments and wire material are analogous to the wire tests, relaxation temperatures and relaxation stresses as well. As before, the four temporal measuring points of the reduced spring force $F(t)$, as well as the curve fits, calculated by means of **equation 7**, are displayed by plotting relaxation loss over relaxation time (for each spring, F_0 is measured at the start of the relaxation tests):

$$\text{Relaxation loss [\%]} = \left(1 - \frac{F(t)}{F_0}\right) * 100\ \% \qquad (9)$$

Figure 9 exemplary depicts relaxation curves of HCS made of 200°C/30min-HT Pb-patented wire ($d = 3$ mm, 1200 MPa pre-setting stress) for all four examined spring indexes at 1000 MPa relaxation stress at various relaxation temperatures. It becomes clear that there is no recognizable influence of the spring index in regard to the relaxation losses at hand. Once again, this

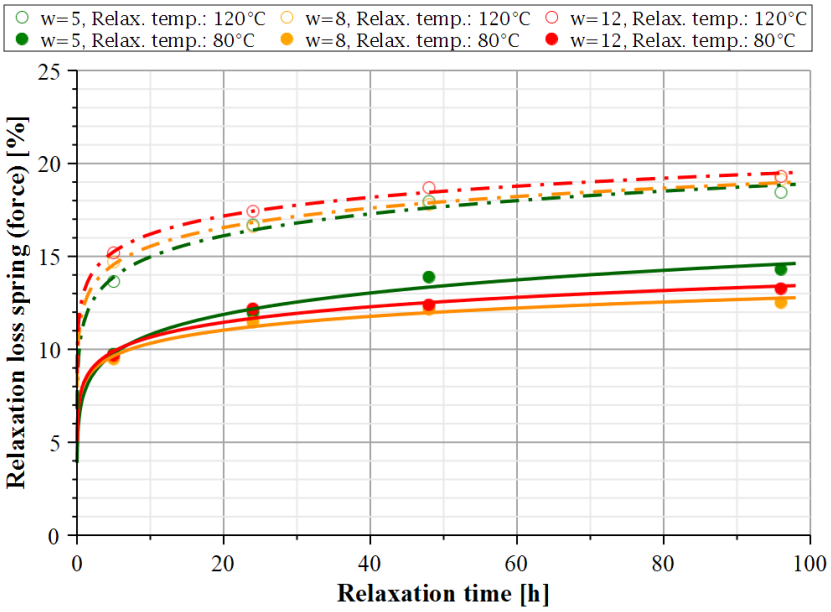

Figure 9:
Relaxation curves of helical compression springs made of **Pb-pat.** wire (d = 3 mm, **200°C/30min** heat-treated, pre-setting stress: 1200 MPa), with various amounts of relaxation temperatures and spring indexes, at **1000 MPa** (uncorrected) **relaxation stress**

observation holds true for all examined types of spring steel wire. The extent of the scatter bands is strongly dependent upon the quality of the measurement points. Occasional outliers are more pronounced in comparison to the wire tests, which can, among other things, be attributed to the more complex geometry of springs as opposed to wires, what makes identical test objects nearly impossible.

5. CREEP SPECIFIC CHARACTERISTICS, GENERAL FINDINGS AND DEDUCTION OF RELAXATION FIGURES

Overall, the creep processes within all examined types of spring steel wires and thereof made helical compression springs could be assigned to the creep mechanism dislocation creep (m = 4, more specific: low temperature creep) as well as to be taking place during the primary creep phase (k < 1). Furthermore, each combination of wire type and heat treatment could be assigned a fix value for k via an iteration process. This represents the prerequisite for the subsequent pictured parametrization of the auxiliary creep parameter c_τ based upon the creep tests with

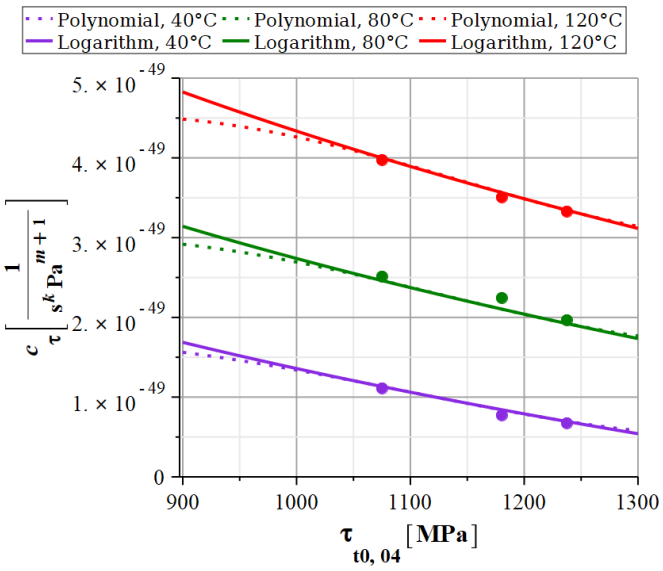

Figure 10:
Creep parameter c_τ with respect to the torsional yield point $\tau_t^*{}_{0,04}$ at various creep temperatures; depicted for multiple basis functions (exemplary for one combination of wire type and heat treatment) [7]

wire. Adapted from the examined levels of pre-torsion stress and creep temperature, correlations with regard to c_τ could be derived, enabling creep deformation to be noted as a function of these parameters in addition to creep time and stress. This was done for each wire type with their respective heat treatment. For one of these, **figure 10** shows c_τ with respect to the torsional yield point of different levels of pre-torsion stress for various creep temperatures and multiple basis functions. The Parametrization of c_τ (**figure 11**) enables the coverage of intermediate ranges between the actual test points during experimentation as well as extrapolation.

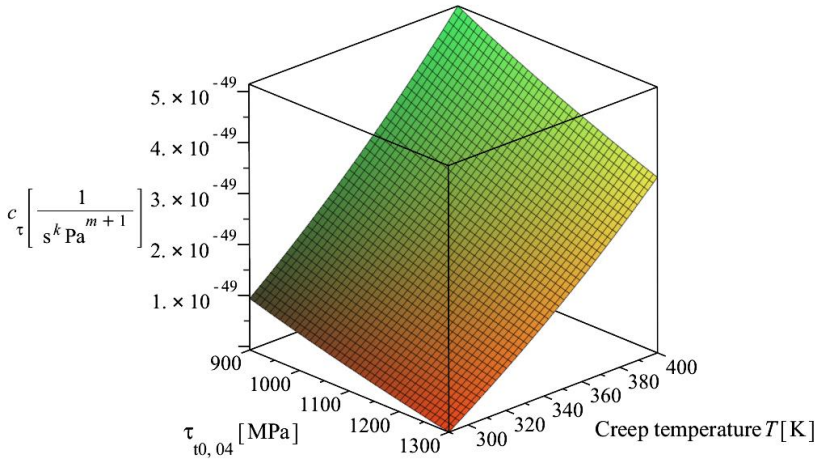

Figure 11:
Creep parameter c_τ as a function of creep temperature and torsional yield point $\tau_t^*{}_{0,04}$ [7]

On the basis of the supplemental relaxation tests (both, with spring steel wire and helical compression springs) transfer factors to adapt creep parameters from one application related to creep processes to another could be determined [8]:

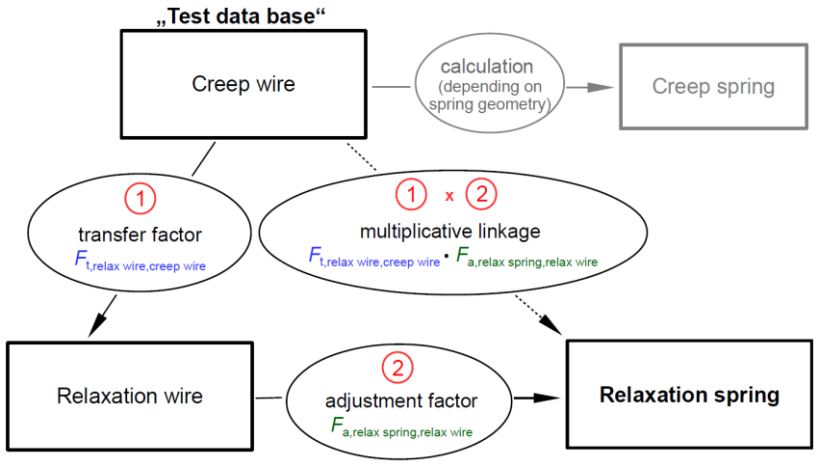

Figure 12:
Procedure to transfer creep parameters characterizing creep of spring steel wires to creep and relaxation of (helical) compression springs [7]

In order to facilitate the practical application of these findings, they were converted into relaxation figures of many different presentations – including but not limited to the depiction in the European standard (48 h relaxation time with respect to relaxation stress). This allows for a better interpretation of those figures and provides an opportunity to grasp deviations when it comes to modern day materials. **Figure 13** contrasts one of these relaxation figures for SiCr-wire (d = 3 mm, HT: 350°C/30min) with the respective curves of the European standard.

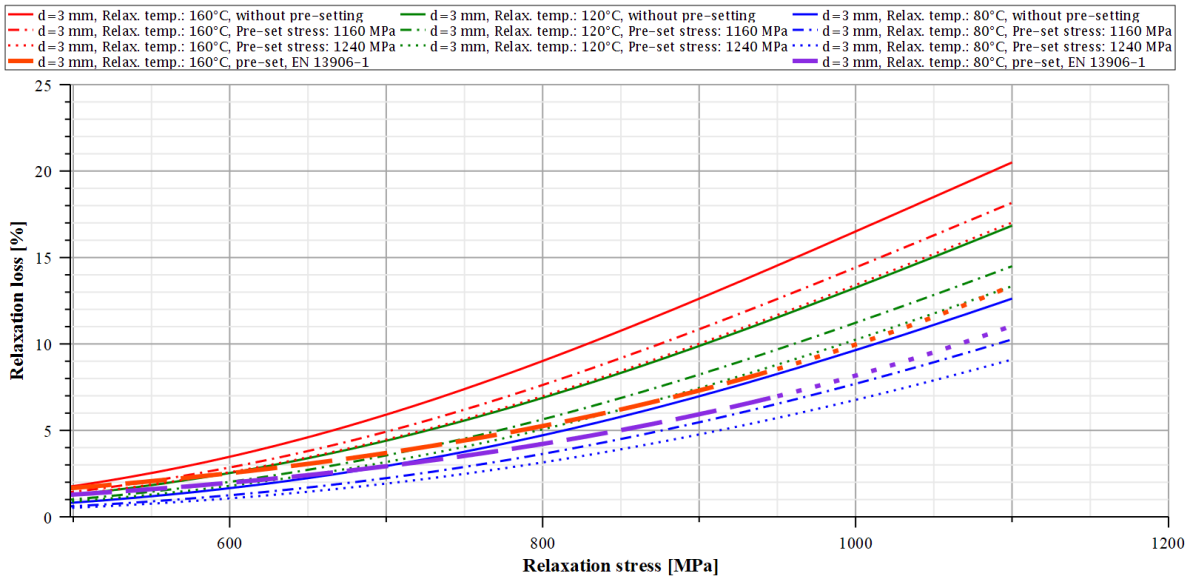

Figure 13: Comparison of relaxation loss from calculated curves (d = 3 mm) as a function of relaxation stress for helical compression springs made of **SiCr** wire, **350°C/30min** heat-treated, after **48h** relaxation time, for various amounts of relaxation temperature; complemented with standard curves

6. CONCLUSION

The experimental examinations have shown that the NORTON-BAILEY creep law is well suited to represent the creep and relaxation behavior of spring steel wires and helical compression springs satisfyingly. The resulting creep parameters suggest the creep mechanism at hand to be dislocation creep ($m = 4$) and locate all creep processes up to 300 h of creep time in the primary creep phase ($k < 1$). As expected, the creep and relaxation losses increase with increasing amounts of creep, respectively relaxation, stress and temperature. With regard to the effect of heat treatment, it can generally be stated that heat treatment has a positive effect on the creep/relaxation behavior of spring steel wires, respectively helical compression springs made therefrom. The same was found to be true for cold pre-setting – though with different magnitude for the individual types of spring steel wire. The relaxation behavior of helical springs could not be found to be dependent upon the spring index.

As far as the individual types of wire are concerned, it has been found that the 420°C/30min HT leads to considerably greater creep/relaxation losses than the 350°C/30min HT in case of SiCr wire. As for Pb-patented wire, the two respective heat treatments are approximately at the same creep/relaxation level, even though 250°C/30min HT results in slightly more pronounced creep/relaxation processes. For both, oil hardened and tempered spring steel wire and patented drawn spring steel wire the wire diameter was found to have an effect on the creep/relaxation behavior – albeit much more pronounced for the patented drawn wire. It was possible to roughly differentiate between "thick" ($d > 5$mm) and "thin" ($d \leq 5$ mm) wires, whereas the thick wires show greater losses.

In the case of the examined 1.4310 wire, the creep/relaxation losses decrease continuously with increasing temperature during the heat treatment: 200°C/30min HT leads to the most distinct creep/relaxation processes, the 400°C/30min HT to the least.

Through parametrization with respect to the influencing variables, relaxation figures as functions of creep time, stress and temperature could be generated that complement and exceed those depicted in the European standard.

Following the initial creep studies, long-term creep tests (appr. 1 year) were carried out, which showed that the creep parameters found work conservatively for extrapolated estimates and are thus useful for long-term considerations as they are often requested in practice.

REFERENCES

[1] DIN EN 13906-1: Cylindrical helical springs made from round wire and bar – Calculation and design – Part 1: Compression springs, November 2013

[2] J. Rösler, H. Harders and M. Bäker, Mechanisches Verhalten der Werkstoffe, 4., revised and extended run, Springer Vieweg, Wiesbaden, 2013

[3] M.F. Ashby and H.J. Frost: Deformation-Mechanism Maps – The Plasticity and Creep of Metals and Ceramics, URL: http://engineering.dartmouth.edu/defmech/ , access date: 20.06.2017

[4] G.B. Graves and M. O'Malley, "Relaxation bei Schraubendruckfedern", Draht 34 – Nr. 3, pp. 109–112, 1983

[5] V. Kobelev: Durability of Springs, Springer International Publishing, Chapter 6, Creep and Relaxation of Springs, 2018

[6] V. Kobelev, "Relaxation and creep in twist and flexure", Multidiscipline Modeling in Materials and Structures 10 – Nr. 3, pp. 304–323, October 2014

[7] J. Schleichert and U. Kletzin: Kriech- und Relaxationsverhalten von Federstahldrähten in Schraubenfedern. Final report of the correspondent AiF-project IGF 18992BR. TU Ilmenau, 2018

CONTACTS

M. Sc. Johannes Schleichert email: johannes.schleichert@tu-ilmenau.de
Prof. Dr.-Ing. Ulf Kletzin email: ulf.kletzin@tu-ilmenau.de